J Mater Sci (2015) 50:4698–4706
DOI 10.1007/s10853-015-9020-2

CO_2 absorption properties of Ti- and Na-doped porous Li_4SiO_4 prepared by a sol–gel process

Maoqiao Xiang[1] · Yingchun Zhang[1] · Ming Hong[1] · Shuyan Liu[1] · Yun Zhang[1] · Hui Liu[1] · Cheng Gu[1]

Received: 27 December 2014 / Accepted: 10 April 2015 / Published online: 21 April 2015

Abstract To improve the carbon dioxide (CO_2) absorption performance of lithium orthosilicate (Li_4SiO_4), tablet-like $Li_4Si_{1-x}Ti_xO_4$ and $Li_{3.9}Na_{0.1}Si_{0.96}Ti_{0.04}O_4$ sorbents with loose and porous texture were prepared by a sol–gel process. The relationship between the Ti doping and volume expansion was studied for the first time. The results indicated that the Ti presence into the Li_4SiO_4 structure inhibited the growth of grains and abated the volume expansion. The X-ray diffraction and scanning electron microscopy results showed that the loose and porous solid solutions with similar phase crystallite but different grain sizes could obtain by heat treatment of precursor at 700 °C. The optimum Ti content of $Li_4Si_{1-x}Ti_xO_4$ seems to be 0.04 of $Li_4Si_{0.96}Ti_{0.04}O_4$. And the CO_2 capture behaviors of $Li_{3.9}Na_{0.1}Si_{0.96}Ti_{0.04}O_4$ were better than $Li_4Si_{0.96}Ti_{0.04}O_4$.

Introduction

It is no secret that the world is getting warmer thanks to carbon dioxide (CO_2), a key anthropogenic greenhouse gas [1]. Hence, CO_2 capture technologies have aroused extensive researches. Hitherto, a number of ways have been developed to decrease CO_2 emissions, for example, wet absorption, dry adsorption, membrane separation, and cryogenic separation. However, these technologies are costly and ineffective since they operate at low temperature [2], i.e., the high-temperature exhaust gas needs a cooling process before removing CO_2, which not only adds input but decreases efficiency. Therefore, high-temperature CO_2 absorbents such as hydrotalcites, calcium oxides, and lithium-containing ceramics, have been considered as alternative adsorbents. Among the various solid sorbents, lithium-containing materials, e.g., Li_2ZrO_3, Li_4SiO_4, Li_2CuO_2, Li_5AlO_4, Li_2SiO_3, $Li_6Zr_2O_7$, and Li_8SiO_6 are suggested to be potential materials [3–6]. In addition, Li_2ZrO_3 and Li_4SiO_4 can theoretically adsorb CO_2 in amounts up to 28.7 and 36.7 wt% at high temperature, respectively. Furthermore, the CO_2 adsorption by Li_4SiO_4 is much faster (about 30 times) than Li_2ZrO_3. Besides, Li_4SiO_4 are lighter and cheaper than Li_2ZrO_3 [7–10]. Consequently, Li_4SiO_4 is suggested to be the most promising solid sorbent at high temperature.

Several researches on the kinetic and sorption mechanism of Li_4SiO_4 have been reported [11–13]. A double-shell mechanism and Avrami–Erofeev kinetic model were proposed to describe the sorption process [3]. Figure 1 shows the double-shell structure for the CO_2 sorption on Li_4SiO_4. According to the model and mechanism, the sorption process is not only controlled by the chemisorption but Li^+ and O^{2-} diffusion. Hence, the whole process can be split into two stages: the rapid reaction and diffusion control. The rapid stage is the reaction of CO_2 molecules and Li_4SiO_4 to form solid Li_2CO_3 and Li_2SiO_3 nuclei on the surface (Fig. 1b). The diffusion control stage is the diffusion of Li^+ and O^{2-} through the Li_2SiO_3 shell covering the unreacted Li_4SiO_4. Therefore, in order to improve the sorption properties, the uptake of rapid stage should be enlarged. Meanwhile, the diffusion resistance should be reduced. Carbonates (e.g., Na_2CO_3, K_2CO_3) have been studied as eutectic melts with the outside Li_2CO_3 shell, which can facilitate CO_2 diffusion throughout the first shell [5, 8, 14]. Furthermore, doping hetero elements can enhance ion mobility and reduce diffusion resistance by

✉ Yingchun Zhang
zycustb@163.com

[1] School of Materials Science and Engineering, University of Science and Technology Beijing, 30 Xueyuan Road, Haidian District, Beijing 100083, People's Republic of China

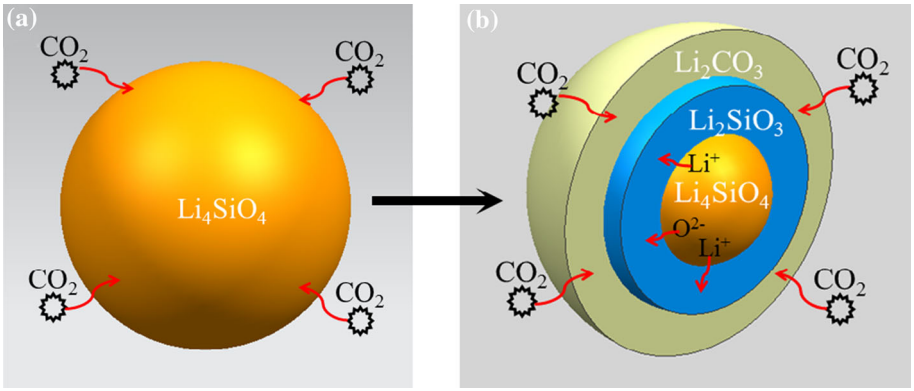

Fig. 1 Illustration of double-shell structure for the CO_2 sorption process on Li_4SiO_4

forming point defects or secondary phases [8]. For example, $Li_{4-x}Na_xSiO_4$ [5], $Li_{3.7}Al_{0.1}SiO_4$, and $Li_{3.7}Fe_{0.1}SiO_4$ [8], $Li_{2-x}Na_xZrO_3$ [15, 16], $Li_{2-x}K_xZrO_3$ [17], $Na_2(Zr_{1-x}Al_x)O_3$ [18], and $Li_{4+x}(Si_{1-x}Al_x)O_4$ [19] showed that even small quantity of a doping component can improve the sorption property [9]. And lithium silicate platelets synthesized by a sol–gel approach had been studied to enhance CO_2 absorption kinetics [20]. Currently most researches focus on introducing Na or K to replace Li element for improving surface chemisorption sorption properties. And the Al, Fe, and V were studied to occupy Si atom [8, 21]. However, there are barely relevant investigations about the relationship of doping and volume expansion, which is extremely important for potential industry application.

As the Ti–O bond is stronger than the Si–O bond [22], the Li–O bond interaction is decreased in Li_4SiO_4 structure when the Si atom is replaced by Ti atom, and then the Li ion conductivity should be improved. Meanwhile, Mejía-Trejo reported that Na-doped Li_4SiO_4 increased the kinetic reaction of CO_2 absorption [5]. Therefore, in this paper, Ti and Na elements were co-doped into Li_4SiO_4 to enhance the sorption properties. The relationship of doping and volume expansion of Li_4SiO_4 was studied. Additionally, the crystal structure, microstructure, sorption, and cyclability of the doped Li_4SiO_4 were investigated.

Materials and methods

Experiment

$Li_4Si_{1-x}Ti_xO_4$ ($x = 0$, 0.005, 0.01, 0.02, 0.04, 0.06) and $Li_{3.9}Na_{0.1}Si_{0.96}Ti_{0.04}O_4$ solid solutions were synthesized by sol–gel process. A flow chart of the process is shown in Fig. 2. Raw materials were lithium nitrate ($LiNO_3$), tetrabutyl titanate ($Ti(OC_4H_9)_4$), tetraethyl orthosilicate ($Si(OC_2H_5)_4$), sodium hydroxide (NaOH), ethanol (CH_3CH_2OH), and citric acid ($C_6H_8O_7$). All the chemicals were analytical reagent grade and purchased from Sinopharm Chemical Reagent Co., Ltd. Firstly, solution of $Ti(OC_4H_9)_4$ and CH_3CH_2OH was added dropwise into a stirring aqueous solution of $LiNO_3$, $C_6H_8O_7$, and CH_3CH_2OH. After the mixed solution became transparent, a solution of $Si(OC_2H_5)_4$ and CH_3CH_2OH was mixed with the transparent solution, and then the solution was heated at 50 °C with continuously stirring for several hours till it became a yellowish dry gel. After that, the dry gel was ground and pressed into about 20 mm diametric tablet and calcined at 700 °C for 4 h.

Characterization techniques

Thermal behaviors of Li_4SiO_4 dry gel were examined by thermogravimetry–differential thermal analysis (TG–DTA) instrument (STA409C NETZSCH, Germany) from room temperature to 800 °C with 10 °C/min under air for determining the sintering temperature. All samples were characterized by powder X-ray diffraction (XRD, D/Max-RB, RB Rigaku, Japan), and the cell parameters were refined by utilizing MDI Jade 5.0 software. The nitrogen adsorption measurements were carried out using Quadrasorb-18, Quantachrome, USA. The morphologies and particle size of the solid solutions were observed by scanning electron microscopy (SEM, JSM-6480LVJEOL, Japan). CO_2 absorption properties of $Li_4Si_{1-x}Ti_xO_4$ ($0 \le x \le 0.06$) and $Li_{3.9}Na_{0.1}Si_{0.96}Ti_{0.04}O_4$ were carried out by TG–DTA instrument (STA409C NETZSCH, Germany) under CO_2 flux. Additionally, the cyclability of $Li_{3.9}Na_{0.1}Si_{0.96}Ti_{0.04}O_4$, $Li_4Si_{0.96}Ti_{0.04}O_4$, and Li_4SiO_4 were measured at 650 °C under CO_2 and N_2 flux (for desorption).

Results and discussions

Characterization

To determine the sintering temperature, TG–DTA curves (Fig. 3) of the Li_4SiO_4 precursor were carried out in air. The curves indicated that the small endothermic peak at

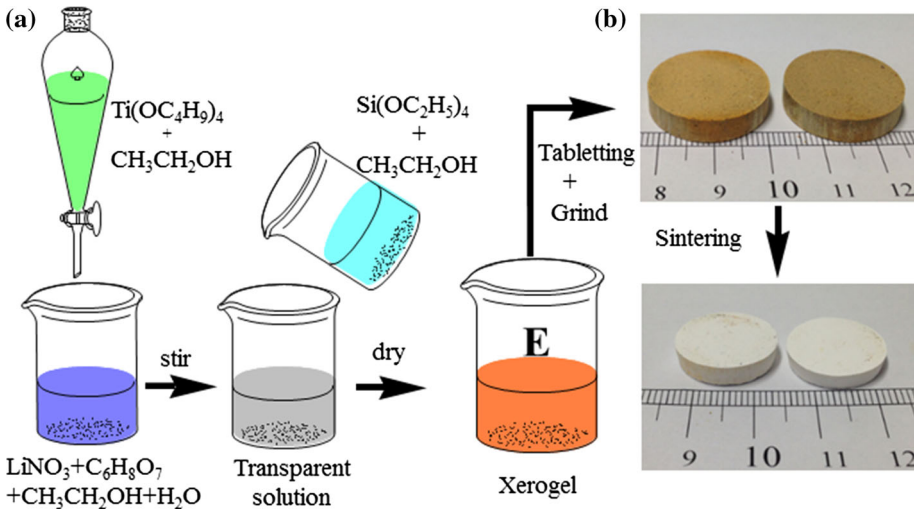

Fig. 2 Flow chart of synthesis of tablet-like $Li_4Si_{1-x}Ti_xO_4$ ($0 \le x \le 0.06$) and $Li_{3.9}Na_{0.1}Si_{0.96}Ti_{0.04}O_4$

about 270 °C might be assigned to the removal of combined water, and two sharp exothermic peaks at about 380 °C and 650 °C could be due to the organics combustion and the Li_4SiO_4 phase formation, respectively. No additional endothermic or exothermic peaks and weight changes were detected above 700 °C, which suggested that the synthesis process had completely finished. Therefore, the $Li_4Si_{1-x}Ti_xO_4$ ($0 \le x \le 0.06$) and $Li_{3.9}Na_{0.1}Si_{0.96}Ti_{0.04}O_4$ dry gel precursor were heat treated at 700 °C for 4 h for further investigation.

After the series samples were synthesized, the samples were characterized by XRD (Fig. 4a). The $x = 0$ (Li_4SiO_4) diffraction pattern fitted very well to the JCPDS file 37–1472 (cell parameters: $a = 5.297$ Å, $b = 6.101$ Å, $c = 5.150$ Å, $\beta = 90.251°$), which manifested that the sol–gel precursor calcined at 700 °C for 4 h could obtain pure Li_4SiO_4 phase. In this experiment, once the Ti addition started, the intensity of diffraction peak weakened with the increase of Ti content. Meanwhile, the diffraction peaks shifted slightly toward lower angles. These effects indicated that titanium doping inhibited the crystallization of Li_4SiO_4. It might be attributed to the difference in ion radius of Si^{4+} (0.42 Å) and Ti^{4+} (0.68 Å) and the closed packed structure of the silicate [23, 24]. In Li_4SiO_4 structure, Si locates in tetrahedral site of oxygen. Hence, if the Ti replaced the Si, the cell parameters of doped Li_4SiO_4 would increase, while diffraction angle would decrease by the Bragg's law ($\lambda = 2d\sin\theta$). Figure 4c showed that the cell parameters (a, b, c, and volume (v)) increased with x value, and the increasing rate of c was bigger than a and b. It implied that Ti might be incorporated into the crystal lattice. However, when the x value was 0.06, tiny amounts of Li_2SiO_3 peaks were detected. Although Li_2SiO_3 absorbs CO_2 as well, the kinetic behavior of CO_2 absorption on Li_2SiO_3 is much slower than that on Li_4SiO_4 [5, 22]. Li_2SiO_3 hardly adsorbed CO_2 below 900 °C [25]. In this case, the doping limitation of Ti into Li_4SiO_4 should be 0.04, $Li_4Si_{0.96}Ti_{0.04}O_4$. Meanwhile, Mejía-Trejo reported that the solubility limit of sodium into Li_4SiO_4 is 0.1, $Li_{3.9}Na_{0.1}SiO_4$ [5]. Hence, NaOH was doped into Li_4SiO_4. In this experiment, Li_4SiO_4 (main phase) and tiny Li_3NaSiO_4 phase were detected (Fig. 4a). We found that the diffraction peaks shifted toward higher angles, and cell parameters a and c decreased about 0.15 and 0.11 %, while the cell parameter b increased about 0.053 %. It indicated that the Na might be incorporated into the crystal lattice, and the difference in atomic radius of Li (2.05 Å) and Na (2.23 Å) might account for the result. In order to understand the sorption process, the samples after absorbing CO_2 at 650 °C for 1 h were examined by XRD (Fig. 4b). Li_2SiO_3 and Li_2CO_3 peaks were found in all absorbed samples and their intensities were stronger with the increase of Ti content. It was ascribed to the fact that the samples absorbed CO_2 to form Li_2SiO_3 and Li_2CO_3, and the reaction may be described as follows.

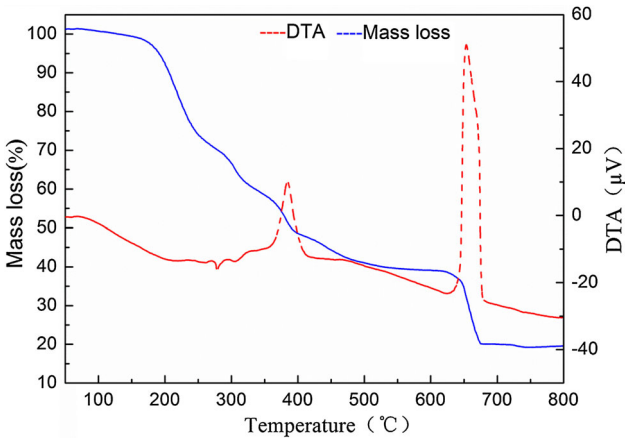

Fig. 3 TG and TDA curves of Li_4SiO_4 dry gel precursor in argon

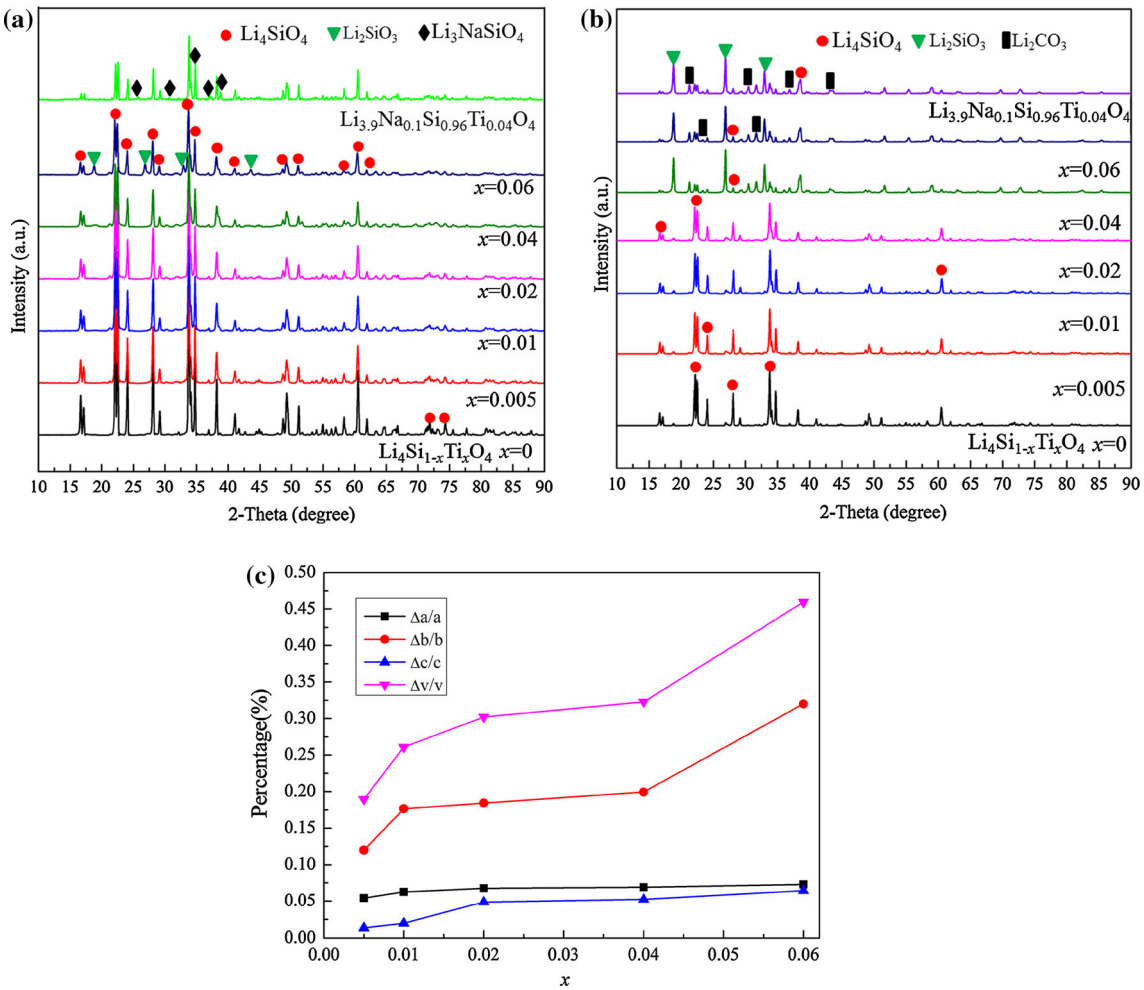

Fig. 4 XRD patterns of $Li_4Si_{1-x}Ti_xO_4$ ($0 \le x \le 0.06$) and $Li_{3.9}Na_{0.1}Si_{0.96}Ti_{0.04}O_4$; **a** before absorption; **b** after absorption; **c** the relationship of cell parameters and x value

$$Li_4SiO_4 + CO_2 \leftrightarrow Li_2SiO_3 + Li_2CO_3 \quad (1)$$

$$Li_4Si_{1-x}Ti_xO_4 + CO_2 \leftrightarrow (1-x)Li_2SiO_3 + Li_2CO_3 + xLi_2TiO_3 \quad (2)$$

$$Li_{3.9}Na_{0.1}Si_{0.96}Ti_{0.04}O_4 + CO_2 \leftrightarrow 0.95Li_2CO_3 + 0.05Na_2CO_3 + 0.96Li_2SiO_3 + 0.04Li_2TiO_3 \quad (3)$$

However, no Na_2CO_3 and Li_2TiO_3 peaks were identified in the XRD patterns as its abundance is beyond the XRD resolution.

The morphologies of the unabsorbed and absorbed samples are shown in Fig. 5. As observed in Fig. 5a, all the unabsorbed tablet samples had a loose and porous microstructure. Table 1 shows the surface area, pore size, and pore volume of $Li_4Si_{1-x}Ti_xO_4$. The surface area and total pore volume increased with x value, and the pore size decreased in some degree, indicating that the dopant would hinder the growth of grains. During sintering process, the combustion products (CO_2 and H_2O steam) of the dry gel precursor moving from the interior to the exterior could be responsible for the loose and porous texture. Knitter reported that Ti doping could enhance the strength of Li_4SiO_4 [22]. Hence, these ceramic pores might offer firm tunnel for CO_2 carriage, which might be better than the tiny and unstable pores of powder adsorbent as the latter may be blocked up after few absorption cycles [18]. In addition, we found that the grain size decreased with Ti content increasing (Fig. 5a). The average size of grains abated from 3 μm (Li_4SiO_4) to 0.23 μm ($Li_4Si_{0.96}Ti_{0.04}O_4$). It seemed that Ti inhibited the growth of the particles, which is consistent with the results of Table 1. Some papers have reported that small particles have high surface area and better chemisorb efficiencies [10, 26, 27]. However,

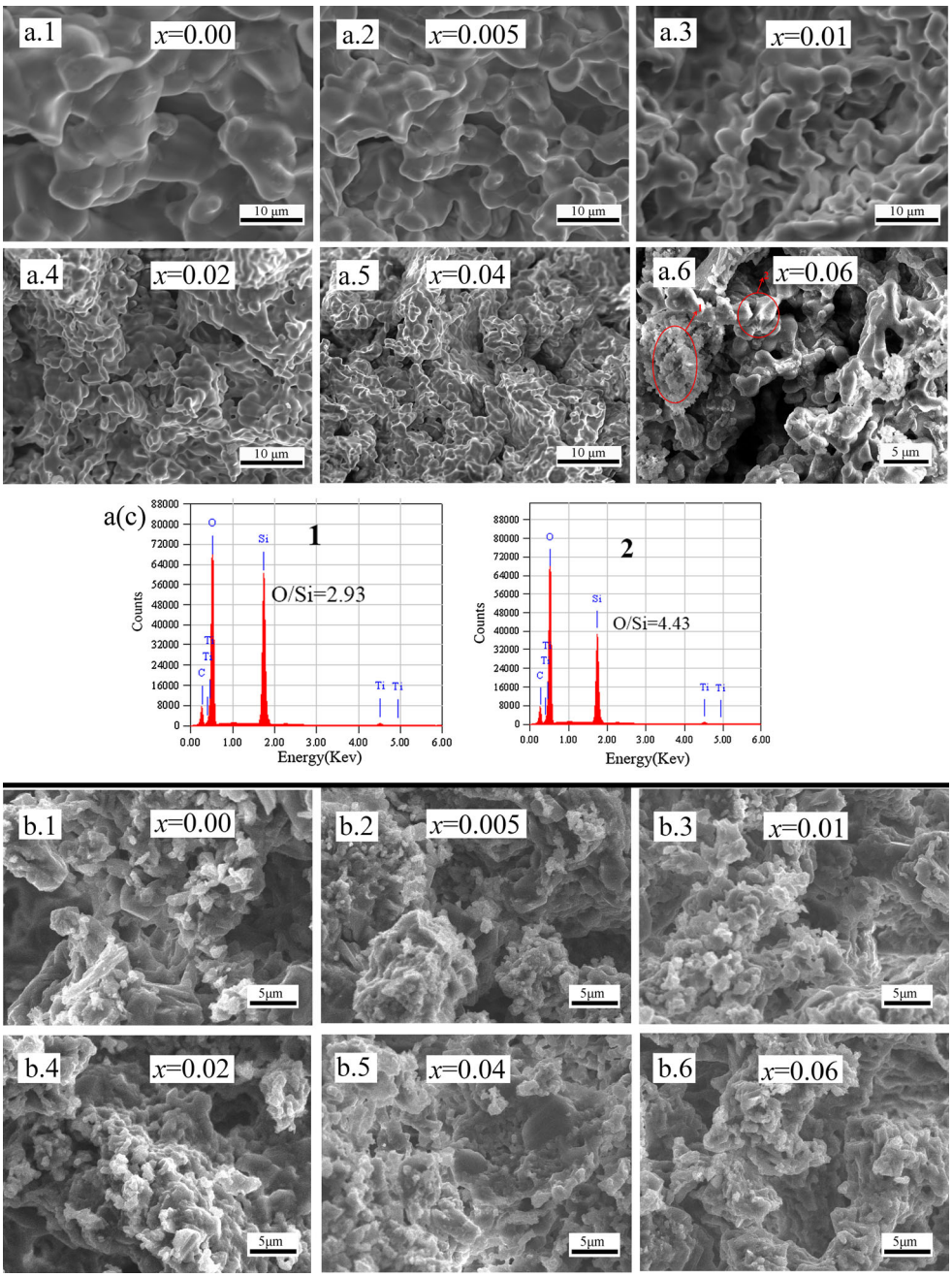

Fig. 5 The microstructure of $Li_4Si_{1-x}Ti_xO_4$ ($0 \le x \le 0.06$); **a** before absorption; **b** after absorption; **c** EDS patterns of $x = 0.06$

Table 1 Parameters of $Li_4Si_{1-x}Ti_xO_4$ ($0 \le x \le 0.06$)

Samples	S_{BET} (m^2/g)	Total pore volume (cm^3/g)	Average pore diameter (nm)
$x = 0$	8.435	0.05013	23.3372
$x = 0.005$	10.056	0.04875	19.3912
$x = 0.01$	11.273	0.04581	16.2235
$x = 0.02$	12.139	0.03827	12.6011
$x = 0.04$	12.767	0.03075	9.6343
$x = 0.06$	13.043	0.02963	9.0778

secondary phase was found in $Li_4Si_{0.96}Ti_{0.06}O_4$, and the EDS images (Fig. 5a(c)) show that the O/Si ratio of the polyhedral shape gray phase was higher (4.43) than the bright dendritic phase (2.93). It indicated that the gray phase and the secondary phase should be Li_4SiO_4 and Li_2SiO_3, respectively, which was also proved by XRD pattern (Fig. 4a). Figure 5b shows the microstructure of the absorbed samples. In all samples, white agglomerate particles covered the light dark phase, and it increased with the x value.

The CO_2 absorbent expansivity α, $\alpha = (M - M_0)/M_0$, where the M and M_0 are the radius (R, R_0), high (H, H_0) or volume (V, V_0) of absorbed and unabsorbed samples, respectively, is extremely important for industry application. In this experiment, we found that the absorption expansion ratio of Li_4SiO_4 was so big that a quartz crucible was cracked by its expansion force. Therefore, the relationship between doping and absorbent expansivity α was investigated for the first time. All samples performed at 650 °C under 160 ml/min CO_2 and 200 ml/min N_2 (desorption gas) for 10 cycles. As can be seen in Fig. 6, the α_R, α_H, and α_V declined sharply as the Ti content increased, and when the $x \geq 0.04$, the α almost reached its limitation. The α_V of Li_4SiO_4 was about 22 %, while the $Li_4Si_{0.96}Ti_{0.04}O_4$ was only about 5.6 %, which almost decreased four times. The stable Ti–O bond can be responsible for these results. Therefore, Ti-doped Li_4SiO_4 could decrease the expansivity.

Investigation of general sorption behavior

The enthalpy changes (ΔH), entropy changes (ΔS), and free energy changes (ΔG) of Li_4SiO_4 absorption reaction were calculated using HSC chemistry 5.11 software (Table 2). Under 720 °C, all ΔG values are <0, revealing that Li_4SiO_4 can absorb CO_2 from room temperature to 720 °C. Figure 7 illustrates the CO_2 sorption behaviors of synthesized samples. All the samples appeared to display similar absorption behaviors. The weight increased slowly from around 200 °C and sharply at about 500 °C. And then it reached a peak at about 650 °C, while over 730 °C the absorption process almost finished. However, around 400 °C, a lightly weight loss was detected. Meanwhile, the weight increased with the x value except $x = 0.06$. To further understand the absorption process, all the samples were tested at 200, 300, 400, 500, 550, and 650 °C under 160 ml/min CO_2 for 3 h (Fig. 8).

As can be seen in Fig. 8, all the weight increased with the x value and temperature except at 400 °C. At relative low temperature (200–400 °C), the increase in tendency showed a linear trend, however, over 500 °C, it increased sharply in a short time to a plateau. These results indicated that the absorption process had two different principles,

Table 2 Calculated ΔH, ΔS, and ΔG for the Li_4SiO_4 absorption reaction

T (°C)	ΔH (KJ)	ΔS (J/K)	ΔG (KJ)
0	−142.215	−165.525	−97.002
100	−140.442	−160.151	−80.682
200	−137.016	−152.085	−65.057
300	−132.12	−142.744	−50.306
400	−124.942	−131.242	−36.596
500	−117.327	−120.518	−24.148
600	−110.88	−112.693	−12.482
700	−103.118	−104.289	−1.629
720	−56.637	−57.466	0.435
800	−50.519	−51.538	4.79

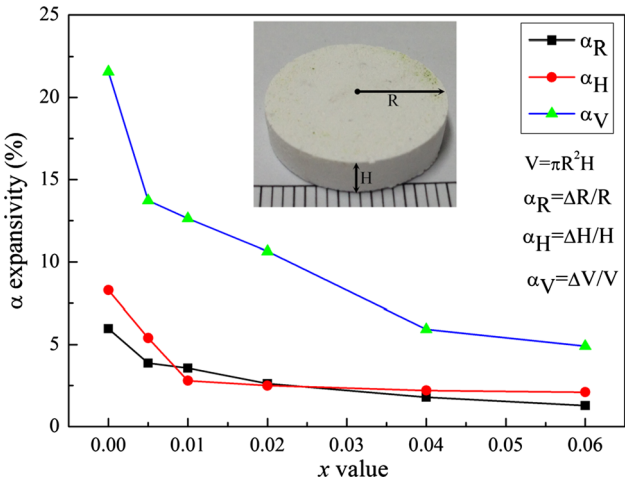

Fig. 6 The relationship between CO_2 absorbent expansivity and Ti doping

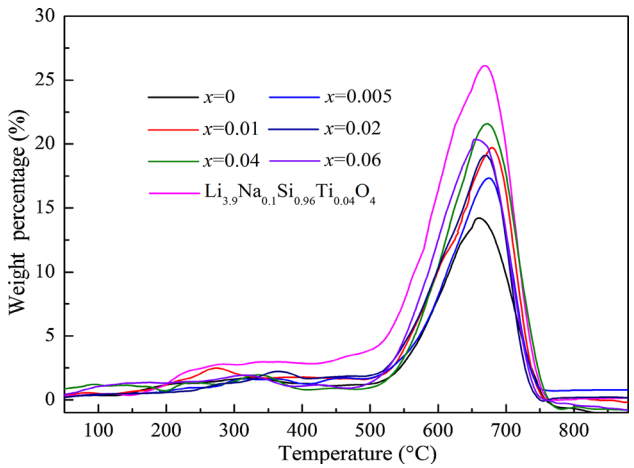

Fig. 7 CO_2 sorption behaviors of $Li_4Si_{1-x}Ti_xO_4$ ($x = 0$, 0.005, 0.01, 0.02, 0.04, and 0.06) and $Li_{3.9}Na_{0.1}Si_{0.96}Ti_{0.04}O_4$ under 160 ml/min CO_2 from room temperature to 880 °C with a heating rate of 10 °C/min

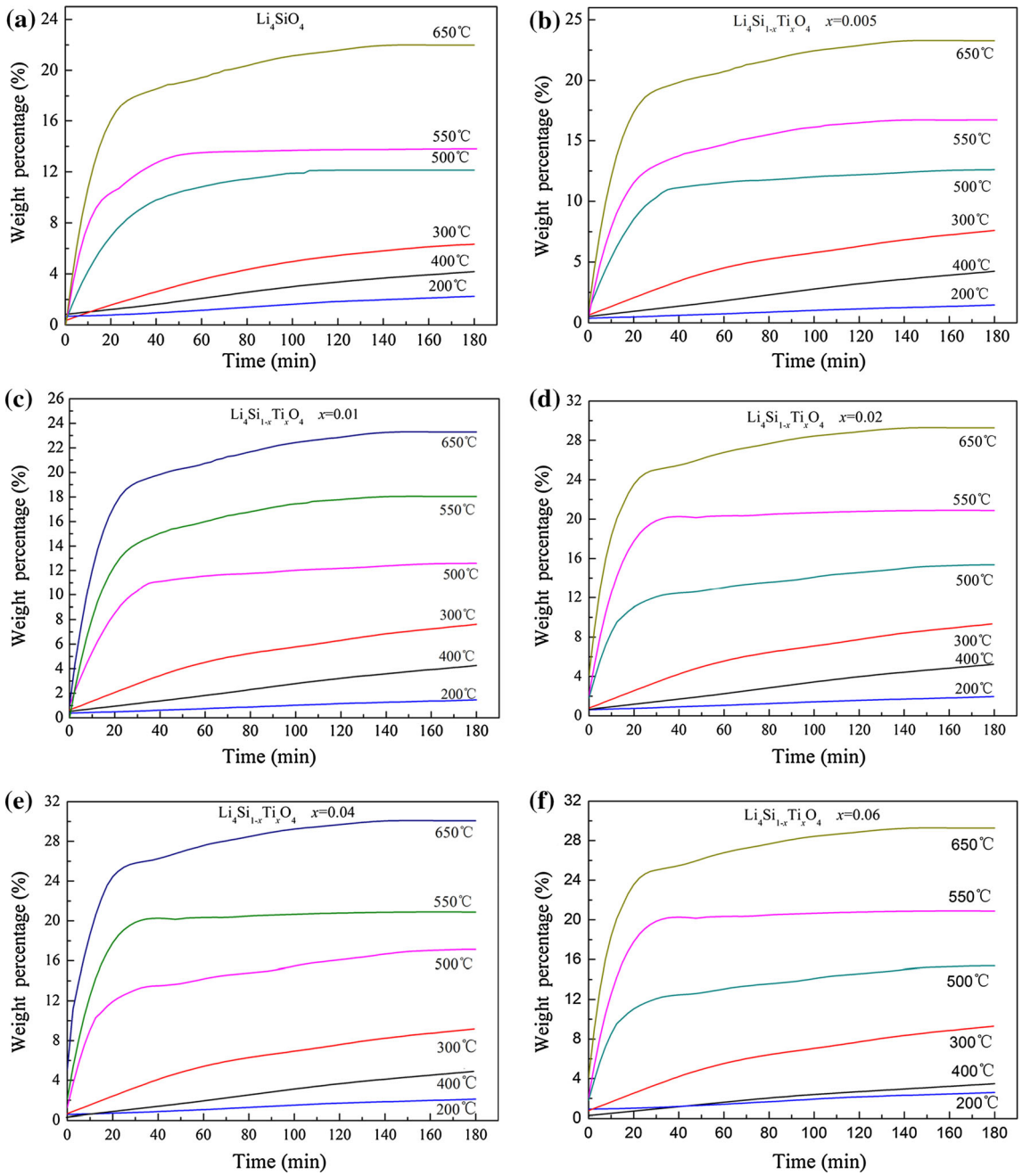

Fig. 8 CO_2 sorption behaviors of $Li_4Si_{1-x}Ti_xO_4$ at 200, 300, 400, 500, 550, and 650 °C under 160 ml/min CO_2

i.e., initially, at relative low temperature, the CO_2 chemisorption occurred over the absorbent surface forming an external shell, which resisted the Li^+, O^{2-}, and CO_2 diffusion and hindered the further reaction [12]. Nevertheless, at high temperature, the chemisorption can be reactivated as the Li^+, O^{2-}, and CO_2 obtained sufficient driving force throughout the bulk of the external shell [5]. However, at 400 °C, the weight was more minor than at 300 °C. Similar behaviors have been reported on $Li_{4-x}(Si_{1-x}Al_x)O_4$ and $Na_2(Zr_{1-x}Al_x)O_3$ at 400 and 300 °C, respectively [18, 21], which further provided evidence for a superficial chemisorption–desorption equilibrium. Therefore, the superficial desorption process does not seem to be modified by the Ti doping. However, it improved the absorption performance. At 300 °C, the weight increased from 7.3 wt% ($x = 0$) to 8.6 wt% ($x = 0.06$). Continuous decreasing grain size caused by Ti doping (Fig. 5a) may account for the changes.

Figure 9 shows $Li_4Si_{1-x}Ti_xO_4$ and $Li_{3.9}Na_{0.1}Si_{0.96}Ti_{0.04}O_4$ absorption performance at 650 °C. As can be seen,

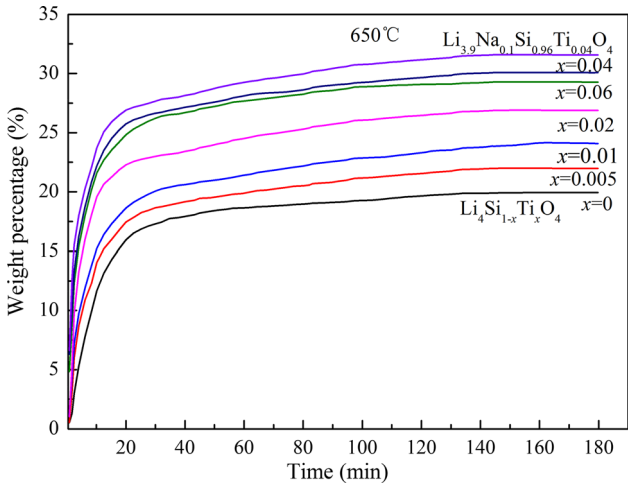

Fig. 9 CO_2 sorption behaviors of $Li_4Si_{1-x}Ti_xO_4$ and $Li_{3.9}Na_{0.1}Si_{0.96}Ti_{0.04}O_4$ at 650 °C under 160 ml/min CO_2

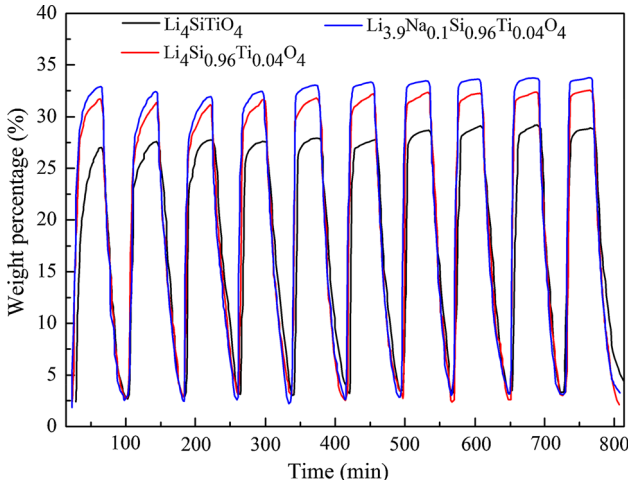

Fig. 10 Multi-cycle performance of CO_2 chemisorption/desorption on Li_4SiO_4, $Li_4Si_{0.96}Ti_{0.04}O_4$, and $Li_{3.9}Na_{0.1}Si_{0.96}Ti_{0.04}O_4$ at 650 °C

$Li_4Si_{0.96}Ti_{0.04}O_4$ and $Li_{3.9}Na_{0.1}Si_{0.96}Ti_{0.04}O_4$ showed a significant improvement on the absorption. It was up to 20.1, 30.4, and 31.6 wt% for Li_4SiO_4, $Li_4Si_{0.96}Ti_{0.04}O_4$, and $Li_{3.9}Na_{0.1}Si_{0.96}Ti_{0.04}O_4$, respectively. For $Li_{4-x}(Si_{1-x}Al_x)O_4$ series, a slight decline was found when $x = 0.06$. The decrement should be attributed to the presence of secondary phase Li_2SiO_3 (Fig. 4a) which is not as good as Li_4SiO_4 in terms of CO_2 absorption kinetic behavior [13, 26]. And the augment of $Li_{4-x}(Si_{1-x}Ti_x)O_4$ series may be due to the enhancement of Li^+ diffusion and the decrease of grain size by doping Ti. For $Li_{3.9}Na_{0.1}Si_{0.96}Ti_{0.04}O_4$, the Ti and Na incorporated into the crystal lattice should be responsible for the augment as they could enhance Li^+ and O^{2-} diffusion by forming lattice distortion (Fig. 4c), dislocations, interstitial atoms, and vacancies. Meanwhile, we found that the chemisorption time at 650 °C, exponential curves reached their plateaus, decreased with x value increasing (15 min, $Li_4Si_{0.96}Ti_{0.04}O_4$) since the grain size diminished (Fig. 5a).

In order to evaluate the regeneration properties and the thermal stability, Li_4SiO_4, $Li_4Si_{0.96}Ti_{0.04}O_4$, and $Li_{3.9}Na_{0.1}Si_{0.96}Ti_{0.04}O_4$ were exposed to CO_2 (160 mL/min) for 1 h and then to N_2 (200 mL/min) for 40 min at 650 °C (Fig. 10). The results indicated that the chemisorption capacity increased with the increasing of cycle numbers. For $Li_{3.9}Na_{0.1}Si_{0.96}Ti_{0.04}O_4$, the chemisorption capacity reached 32.5 wt% for the first cycle, and after 10 cycles it stabilized at 33.1 wt%. In contrast, for Li_4SiO_4 and $Li_{3.9}Na_{0.1}Si_{0.96}Ti_{0.04}O_4$, the chemisorption, after 10 cycles, stabilized to 29.2 and 32.6 wt%. Therefore, $Li_{3.9}Na_{0.1}Si_{0.96}Ti_{0.04}O_4$ had better regeneration properties due to Na and Ti co-doping. However, in the first two and three cycles, a slightly decrement was detected. A particle sintering effect may account for these changes as it decreased the surface area [18]. Meanwhile, we found that the saturate time slightly decreased with cycle numbers. These behaviors may be related to the decreased grains as the chemisorption produced tiny agglomerate lithium-containing oxide particles (Fig. 5b).

It is worth mentioning that all the samples for absorption performance testes were in the form of pills. Hence, the loose and porous $Li_{3.9}Na_{0.1}Si_{0.96}Ti_{0.04}O_4$ pills prepared by sol–gel process could be used as a high-temperature CO_2 absorbent.

Conclusions

Tablet-like $Li_4Si_{1-x}Ti_xO_4$ and $Li_{3.9}Na_{0.1}Si_{0.96}Ti_{0.04}O_4$ sorbents were prepared by a sol–gel process. The analysis performed by XRD suggests that Ti and Na are incorporated to the Li_4SiO_4 structure, and the solubility limit of Ti was 0.04, $Li_4Si_{0.96}Ti_{0.04}O_4$. The SEM analysis indicated that the Ti doping not just decreased the grain sizes but abated the volume expansion of pure Li_4SiO_4. $Li_4Si_{1-x}Ti_xO_4$ and $Li_{3.9}Na_{0.1}Si_{0.96}Ti_{0.04}O_4$ were able to chemisorb CO_2 from 200 to 700 °C, exhibiting higher CO_2 absorption performance than pure Li_4SiO_4. The isothermal analyses suggested that the absorption process had two principles: (1) the chemisorption occurred over the absorbent surface forming an external shell at low temperature phase (200–400 °C), (2) the chemisorption controlled by Li^+, O^{2-}, and CO_2 diffusion processes. The absorption capacities of Li_4SiO_4 at 650 °C, 30.4 and 31.6 wt% for $Li_4Si_{0.96}Ti_{0.04}O_4$ and $Li_{3.9}Na_{0.1}Si_{0.96}Ti_{0.04}O_4$, respectively, were improved by Ti doping and Na and Ti co-doping. The augments could be attributed to that Ti and Na incorporated into the crystal lattice and enhanced Li^+ and O^{2-} diffusion.

The cyclic experiments indicated that $Li_{3.9}Na_{0.1}Si_{0.96}Ti_{0.04}O_4$ exhibited better CO_2 capture behaviors than $Li_4Si_{0.96}Ti_{0.04}O_4$.

Acknowledgements This work has been financially supported by the National Natural Science Foundation of China (Nos. 51372017 and 51172019) and International Thermonuclear Experimental Reactor (ITER) Project of China (No. 2014GB123000).

References

1. Xu H, Cheng W, Jin X (2013) Effect of the particle size of quartz powder on the synthesis and CO_2 absorption properties of Li_4SiO_4 at high temperature. Ind Eng Chem Res 52(5):1886–1891
2. Seggiani M, Puccini M, Vitolo S (2011) High-temperature and low concentration CO_2 sorption on Li_4SiO_4 based sorbents: study of the used silica and doping method effects. Int J Greenh Gas Control 5(4):741–748
3. Qi Z, Daying H, Yang L (2013) Analysis of CO_2 sorption/desorption kinetic behaviors and reaction mechanisms on Li_4SiO_4. AIChE J 59(3):901–911
4. Nair BN, Burwood RP, Goh VJ (2009) Lithium based ceramic materials and membranes for high temperature CO_2 separation. Prog Mater Sci 54(5):511–541
5. Mejía-Trejo VL, Fregoso-Israel E, Pfeiffer H (2008) Textural, structural, and CO_2 chemisorption effects produced on the lithium orthosilicate by its doping with sodium ($Li_{4-x}Na_xSiO_4$). Chem Mater 20(22):7171–7176
6. Radfarnia HR, liuta MCI (2011) Surfactant-template/ultrasound-assisted method for the preparation of porous nanoparticle lithium zirconate. Ind Eng Chem Res 50(15):9295–9305
7. Kato M, Yoshikawa S, Nakagawa KJ (2002) Carbon dioxide absorption by lithium orthosilicate in a wide range of temperature and carbon dioxide concentrations. J Mater Sci Lett 21(16):485–487
8. Gauer C, Heschel W (2006) Doped lithium orthosilicate for absorption of carbon dioxide. J Mater Sci 41(8):2405–2409. doi:10.1007/s10853-006-7070-1
9. Ida JI, Xiong R, Lin YS (2004) Synthesis and CO_2 sorption properties of pure and modified lithium zirconate. Sep Purif Technol 36(1):41
10. Xiong R, Ida J, Lin YS (2003) Kinetics of carbon dioxide sorption on potassium-doped lithium zirconate. Chem Eng Sci 58(19):4377–4385
11. Essaki K, Kato M, Nakagawa K (2006) CO_2 removal at high temperature using pace bed of lithium silicate pellets. J Ceram Soc Jpn 114(9):739–742
12. Rodrıguez-Mosqueda R, Pfeiffer H (2010) Thermokinetic analysis of the CO_2 chemisorption on Li_4SiO_4 by using different gas flow rates and particle sizes. J Phys Chem A 114(13):4535–4541
13. Venegas MJ, Fregoso-Israel E, Escamilla R (2007) Kinetic and reaction mechanism of CO_2 sorption on Li_4SiO_4: study of the particle size effect. Ind Eng Chem Res 46(8):2407–2412
14. Zhang S, Zhang Q, Wang H (2014) Absorption behaviors study on doped Li_4SiO_4 under a humidified atmosphere with low CO_2 concentration. Int J Hydrogen Energy 39(31):17913–17920
15. Pfeiffer H, Lima E, Bosch P (2006) Lithium-Sodium metazirconate solid solutions, $Li_{2-x}Na_xZrO_3$ ($0 \leq x \leq 2$): a hierarchical architecture. Chem Mater 18(11):2642–2647
16. Pfeiffer H, Vazquez C, Lara VH, Bosch P (2007) Thermal behavior and CO_2 absorption of $Li_{2-x}Na_xZrO_3$ solid solutions. Chem Mater 19(4):922–926
17. Veliz-Enriquez MY, Gonzalez G, Pfeiffer H (2007) Synthesis and CO_2 capture evaluation of $Li_{2-x}K_xZrO_3$ solid solutions and crystal structure of a new lithium–potassium zirconate phase. J Solid State Chem 180(9):2485–2492
18. Alcántar-Vázquez B, Diaz C, Romero-Ibarra IC (2013) Structural and CO_2 chemisorption analyses on $Na_2(Zr_{1-x}Al_x)O_3$ solid solutions. J Phys Chem C 117(32):16483–16491
19. Ortiz-Landeros J, Romero-Ibarra IC, Gómez-Yáñez C (2013) $Li_{4+x}(Si_{1-x}Al_x)O_4$ Solid solution mechanosynthesis and kinetic analysis of the CO_2 chemisorption process. J Phys Chem C. 117(12):6303–6311
20. Subha PV, Nair BN, Hareesh P (2014) Enhanced CO_2 absorption kinetics in lithium silicate platelets synthesized by a sol–gel approach. J Mater Chem A 2(32):12792–12798
21. Ortiz-Landeros J, Gómez-Yáñez C, Palacios-Romero LM (2012) Structural and thermochemical chemisorption of CO_2 on $Li_{4+x}(Si_{1-x}Al_x)O_4$ and $Li_{4-x}(Si_{1-x}V_x)O_4$ solid solutions. J Phys Chem A 116(12):3163–3171
22. Knitter R, Kolb MHH, Kaufmann U (2013) Fabrication of modified lithium orthosilicate pebbles by addition of titania. J Nucl Mater 442(1):S433–S436
23. Huheey JE (1981) Inorganic Chemistry, 2nd edn. Harper and Row, New York
24. Cotton FA, Wilkinson G (2001) Advanced inorganic chemistry, 9th edn. Limusa Noriega, Mexico
25. Duan Y, Pfeiffer H, Li B (2013) CO_2 capture properties of lithium silicates with different ratios of Li_2O/SiO_2: an ab initio thermodynamic and experimental approach. Phys Chem Chem Phys 15(32):13538–13558
26. Khomane RB, Sharma BK, Saha S (2006) Reverse microemulsion mediated sol–gel synthesis of lithium silicate nanoparticles under ambient conditions: scope for CO_2 sequestration. Chem Eng Sci 61(10):3415–3418
27. Choi KH, Korai Y, Mochida I (2003) Preparation of CO_2 absorbent by spray pyrolysis. Chem Lett 32(10):924–925